
Article:
Kaiser, Daniel orcid.org/0000-0002-9007-3160, Azzalini, Damiano C and Peelen, Marius V (2016) Shape-independent object category responses revealed by MEG and fMRI decoding. Journal of Neurophysiology. pp. 2246-50. ISSN 0022-3077

https://doi.org/10.1152/jn.01074.2015

Shape-independent object category responses revealed by MEG and fMRI decoding

Daniel Kaiser[1,*], Damiano C. Azzalini[1,*], Marius V. Peelen[1]

Center for Mind/Brain Sciences, University of Trento, 38068 Rovereto (TN), Italy

**D.K. and D.C.A. contributed equally to this study*

Corresponding Author

Marius V. Peelen

Center for Mind/Brain Sciences, University of Trento

Corso Bettini 31, 38068 Rovereto (TN), Italy

Phone: +39 0464 808718, e-mail: marius.peelen@unitn.it

Running Head

Decoding shape-independent object category responses

Author Contributions

D.K., D.C.A., and M.V.P. conception and design of research; D.K. and D.C.A. performed experiments; D.K. and D.C.A. analysed data; D.K., D.C.A., and M.V.P. interpreted results of experiments; D.K. prepared figures; D.K. and M.V.P. drafted manuscript; D.K., D.C.A. and M.V.P. edited and revised manuscript; D.K., D.C.A. and M.V.P. approved final version of manuscript.

Abstract

Neuroimaging research has identified category-specific neural response patterns to a limited set of object categories. For example, faces, bodies, and scenes evoke activity patterns in visual cortex that are uniquely traceable in space and time. It is currently debated whether these apparently categorical responses truly reflect selectivity for categories or instead reflect selectivity for category-associated shape properties. In the present study, we used a cross-classification approach on fMRI and MEG data to reveal both category-independent shape responses and shape-independent category responses. Participants viewed human body parts (hands and torsos) and pieces of clothing that were closely shape-matched to the body parts (gloves and shirts). Category-independent shape responses were revealed by training multivariate classifiers on discriminating shape within one category (e.g., hands versus torsos) and testing these classifiers on discriminating shape within the other category (e.g., gloves versus shirts). This analysis revealed significant decoding in large clusters in visual cortex (fMRI), starting from 90ms after stimulus onset (MEG). Shape-independent category responses were revealed by training classifiers on discriminating object category (bodies, clothes) within one shape (e.g., hands versus gloves) and testing these classifiers on discriminating category within the other shape (e.g., torsos versus shirts). This analysis revealed significant decoding in bilateral occipitotemporal cortex (fMRI), and from 130 to 200ms after stimulus onset (MEG). Together, these findings provide evidence for concurrent shape and category selectivity in high-level visual cortex, including category-level responses that are not fully explicable by 2D shape properties.

Keywords: Category Selectivity, Visual Cortex Organization, Body Representations

45 **Introduction**

46 Functional magnetic resonance imaging (fMRI) studies have shown that multi-voxel
47 response patterns in high-level visual cortex reliably discriminate different object
48 categories (Haxby et al., 2001), and that these show a meaningful categorical
49 organization (e.g., an animate-inanimate distinction; Kriegeskorte et al., 2008). Similarly,
50 signatures of category-specific processing in the time domain have been identified using
51 magneto- and electroencephalography (MEG/EEG), with MEG sensor patterns across the
52 scalp allowing for reliable classification of object categories (Carlson et al., 2013; Cichy et
53 al., 2014).

54 However, it is unclear whether such categorical responses are truly reflecting
55 category membership, detached from specific visual features, or whether they are
56 instead driven by visual properties of objects that systematically covary with category
57 membership. For example, the face-selective fusiform face area (Kanwisher et al., 1997)
58 is preferentially activated for round, non-face stimuli that have a higher spatial
59 concentration of elements in the upper half even when these stimuli are not recognized
60 as faces (Caldara et al., 2006), and the occipital face area (Gauthier et al., 2000) has been
61 shown to be causally involved in the perception of stimulus symmetry (Bona et al., 2015).
62 Furthermore, large-scale response patterns in monkey IT can be well explained by the
63 objects' shape similarity without the need to refer to category membership (Baldassi et
64 al., 2013). Such findings prompt the hypothesis that closely matching shape properties of
65 objects from different categories would largely abolish category-specific response
66 patterns.

67 We tested this prediction by investigating how matching for 2D shape properties
68 impacts neural responses to a specific category -- the human body. Previous studies have

characterized distinct spatio-temporal signatures of body perception, recruiting specific regions in occipitotemporal and fusiform cortices and evoking specific electrophysiological waveform components (for review, see Peelen and Downing, 2007). Furthermore, bodies can be reliably separated from other categories based on MEG and fMRI response patterns (Cichy et al., 2014; Kriegeskorte et al., 2008). It is unknown whether these body-specific fMRI and MEG responses reflect selectivity for particular shape properties of bodies (e.g., symmetry) or whether they reflect, at least partly, a truly categorical response.

Participants were tested in separate fMRI and MEG experiments with largely identical experimental procedures. Multivariate classification techniques were used to characterize category representations in space (fMRI) and time (MEG). The stimulus set consisted of human body parts (hands and torsos) and pieces of clothing (gloves and shirts) that were closely shape-matched to the body part stimuli. To reveal category-independent shape responses, classifiers were trained to discriminate between different shapes within one category (e.g., hands versus torsos), and tested to discriminate these shapes within the other category (e.g., gloves versus shirts). To reveal shape-independent category responses, classifiers were trained to discriminate between the categories (bodies, clothes) within one shape (e.g., hands versus gloves), and tested to discriminate these categories within the other shape (e.g., torsos versus shirts).

Materials & Methods

Participants. Twenty-four healthy adults (11 male; mean age 24.2 years, SD=3.4) took part in the fMRI experiment and 21 healthy adults (14 male; mean 25.0 years, SD=3.2) took part in the MEG experiment. One participant completed both experiments. All participants had normal or corrected-to-normal visual acuity. All procedures were carried out in accordance with the Declaration of Helsinki and were approved by the ethical committee of the University of Trento.

Stimuli and Procedure. Unless otherwise noted, all aspects of the design were identical between the fMRI and MEG experiments. The full stimulus set consisted of nine different categories (hands, gloves, torsos, shirts, brushes, pens, trees, vegetables, and chairs), with 21 different exemplars per category. Four of these categories (brushes, pens, trees, vegetables) were related to a different research question, and are not analyzed here. Chairs served as target stimuli (see Fig. 1b), and were also excluded from all analyses. Our analyses were focused on the comparison between stimuli depicting human body parts (human hands and torsos, i.e. shirts with a human upper body inside) and stimuli depicting solely pieces of clothing despite being very similar to the human body parts in their shape properties (gloves and shirts; Fig. 1a).

>> *Figure 1* <<

Both experiments consisted of multiple runs, where participants viewed grey-scale images of the different categories for 500ms in a randomized order (see Fig. 1b), with stimuli being separated by a fixation interval varying randomly between 1500 and 2000ms (in discrete steps of 50ms). Participants were instructed to maintain central

fixation and press the response button whenever they saw a chair (these trials appeared equally often as all other categories, e.g., 21 times per run). For the MEG experiment, participants were additionally instructed to specifically use the chair trials for eye blinks. Each run contained each individual exemplar of every category exactly once, leading to a total of 189 trials per run and an average run duration of 7.1 minutes. In the fMRI experiment, every run additionally contained a 10s fixation period at the beginning and end. During the fMRI experiment, participants completed six of these runs (for one participant only data from five runs was collected due to a technical problem), and during the MEG experiment, participants completed ten runs (one participant performed eleven runs). Stimulus presentation was controlled using the Psychtoolbox (Brainard, 1997); in the MRI stimuli were back-projected onto a screen at the end of the scanner bore and participants saw the stimulation through a tilted mirror mounted on the head coil, while in the MEG, stimuli were back-projected onto a translucent screen located in front of the participant.

fMRI data acquisition and preprocessing. MR imaging was conducted using a Bruker BioSpin MedSpec 4T head scanner (Bruker BioSpin, Rheinstetten, Germany), equipped with an eight-channel head coil. During the experimental runs, T2*-weighted gradient-echo echo-planar images (EPI) were collected (repetition time TR=2.0s, echo time TE=33ms, 73° flip angle, 3 x 3 x 3mm voxel size, 1mm gap, 34 slices, 192mm field of view, 64×64 matrix size). Additionally, a T1-weighted image (MPRAGE; 1 x 1 x 1mm voxel size) was obtained as a high-resolution anatomical reference. All resulting data were preprocessed using MATLAB and SPM8. The functional volumes were realigned and coregistered to the structural image. Additionally, structural images were spatially normalized to the MNI-305 template (as included in SPM8), to obtain normalizing

parameters for each participant. These parameters were later used to normalize individual participants' searchlight result maps before entering them into statistical analysis.

fMRI decoding analysis. Multivariate pattern analysis (MVPA) was carried out on a TR-based level using the CoSMoMVPA toolbox (www.cosmomvpa.org). To reveal areas yielding above chance decoding throughout the brain, a searchlight analysis was conducted, where a spherical neighborhood of 40 voxels (6.4mm average radius) was moved across the whole brain. For each voxel belonging to a specific neighborhood, TRs corresponding to the conditions of interested were selected by shifting the voxel-wise time-course of activation by three TRs (to account for the hemodynamic delay). Subsequently, for each run separately, activation values were extracted from the unsmoothed EPI-volumes for each TR coinciding with the onset of a specific condition. Similar to the MEG analysis, MVPA was done in a pairwise fashion: Linear discriminant analysis (LDA) classifiers were trained to discriminate response patterns for two conditions in all but one runs and were subsequently tested on response patterns for these two conditions taken from the remaining, left-out run. This procedure was repeated, so that every run served as the testing set once. For the cross-decoding analysis, classifiers were trained on discriminating two conditions (e.g. hands versus gloves), and tested on two different conditions (e.g. torsos versus shirts); thus, for this analysis, all available trials were used in the training and test set. Pairwise classification accuracy for every voxel was assessed by comparing the labels predicted by the classifier to the actual labels, with chance performance always being 50%. Individual-subject searchlight maps were normalized to MNI-space before they were entered into statistical analyses. Above-chance classification was identified using a threshold-free cluster

enhancement (TFCE) procedure (Smith and Nichols, 2009), where the observed decoding accuracy was tested against a simulated null-distribution (generated from 10,000 bootstrapping iterations). The resulting statistical maps were thresholded at $p < 0.05$ (one-tailed).

MEG acquisition and preprocessing. Electromagnetic brain activity was recorded using an Elekta Neuromag 306 MEG system (Elekta Neuromag® systems, Helsinki, Finland), composed of 204 planar gradiometers and 102 magnetometers. Signals were sampled continuously at 1000 Hz and band-pass filtered online between 0.1 and 330Hz. Offline preprocessing was done using MATLAB and the fieldtrip analysis package (Oostenveld et al., 2011). Data were concatenated for all runs, high-pass filtered at 1Hz, and epoched into trials ranging from -100 to 500ms with respect to stimulus onset. Based on visual inspection, trials containing eye blinks and other movement-related artifacts were completely discarded from all analyses. Data was then baseline-corrected with respect to the pre-stimulus window and downsampled to 100 Hz to increase the signal-to-noise ratio of the multivariate classification analysis (see Carlson et al., 2013).

MEG decoding analysis. MVPA was carried out on single trial data using the CoSMoMVPA toolbox (www.cosmomvpa.org). Only magnetometers were used, as these sensors allowed for the most reliable classification in previous work in our lab (Kaiser et al., 2015). Classification was performed using LDA classifiers. For the shape cross-decoding analysis, classifiers were trained on one category-matched shape comparison (i.e., hands versus torsos or gloves versus shirts) and tested on the other comparison (i.e., gloves versus shirts or hands versus torsos). For the category cross-decoding analysis, classifiers were trained on one shape-matched category comparison (i.e., hands versus gloves or torsos versus shirts) and tested on the other comparison (i.e., torsos

versus shirts or hands versus gloves). To increase the reliability of the data supplied to the classifiers, new, "synthetic" trial data was created by averaging single trial data separately for every condition and chunk, by randomly picking 25% of trials and averaging this data across trials. This procedure was repeated 100 times (with the constraint that no trial was used more than one time more often than any other trial), so that for every condition and chunk, 100 of these synthetic trials were available for classification. Classification accuracy was then assessed by computing the percentage of correctly classified trials in the test chunk, with chance performance being 50%. Classification was repeated for every possible combination of training and testing time points, leading to a 60 X 60 time points (600 X 600ms, with 100Hz temporal resolution) matrix of classification accuracies. Individual subject accuracy maps were smoothed using a 3 X 3 time points (i.e. 30ms in train and test time) averaging filter. To identify time periods of significant above-chance classification, similar to the fMRI analysis, a TFCE procedure was used, where the observed decoding accuracy was tested against a simulated null-distribution (generated from 10,000 bootstrapping iterations). The baseline (pre-stimulus) interval was not taken into account for statistical testing. The resulting statistical maps were thresholded at $p < 0.05$ (one-tailed).

Results

Shape Cross-Decoding. Brain regions representing object shape across categories were identified by training classifiers on discriminating shape within one category (e.g., hands versus torsos), and testing these classifiers on discriminating shape within the other category (e.g., gloves versus shirts). Results from both possible train/test-directions were averaged. An fMRI searchlight using this approach revealed regions in right (33,128mm³; peak MNI coordinate: x=48, y=-68, z=-4; t_{23}=8.5) and left (30,368mm³; peak MNI coordinate: x=-6, y=-94, z=-12; t_{23}=9.6) visual cortex, spanning early visual areas and regions of lateral occipitotemporal cortex (Fig. 2a,b). The MEG data showed above-chance decoding of shape, starting at 90ms after stimulus onset, and peaking along the diagonal at 170ms and 240ms (467 time points in total, maximum decoding accuracy: 70.2%; t_{20}=11.4; Fig. 2c).

>> Figure 2 <<

Category Cross-Decoding. A second cross-decoding analysis was conducted to test for responses that reflect object category (body parts versus clothes), independently of shape properties. To detect such shape-independent responses, classifiers were trained to discriminate bodies and clothes for one shape-matched comparison (e.g., hand versus glove), and subsequently tested on the other comparison (e.g., torso versus shirt). Results from both possible train/test-directions were averaged.

>> Figure 3 <<

In the fMRI searchlight analysis, clusters in right (3,664mm³; peak MNI coordinate: x=52, y=-70, z=6; t_{23}=6.5) and left (5,752mm³; peak MNI coordinate: x=-44, y=-78, z=10; t_{23}=5.8) lateral occipitotemporal cortex were identified (Fig. 3a). These clusters overlapped with the extrastriate body area (EBA; Fig. 3b; coordinates of Downing et al., 2001: x=+/-51, y=-72, z=5). Performing the same cross-classification analysis on the MEG data revealed a specific temporal signature associated with shape-independent category responses: classifiers could reliably discriminate between bodies and clothes between 130–160ms with respect to the hand-glove comparison and 160–200ms with respect to the torso-shirt comparison (12 time points in total, maximum decoding accuracy: 53.6%; t_{20}=6.9; Fig. 3c).

Discussion

Here we asked whether categorical representations in visual cortex are fully driven by category-associated visual features or if they (at least partly) reflect category membership. Unlike previous studies investigating category selectivity, the stimuli presented in the current study were matched for shape properties, including object-part structure (e.g. hands and gloves both have five "fingers"), outline similarity, and symmetry. We found that large clusters in visual cortex are sensitive to shape differences (i.e., “hand/glove”-shape versus “upper body”-shape): classifiers trained on discriminating hands and torsos successfully discriminated gloves and shirts (and vice versa), in both early visual areas and occipitotemporal cortex. These shape differences were reliably decodable from MEG response patterns as early as 90ms after stimulus onset.

Crucially, we also found evidence for shape-independent category responses: classifiers trained on discriminating hands and gloves successfully discriminated torsos and shirts (and vice versa) in bilateral clusters in the occipitotemporal cortex. These large clusters likely encompass body-, motion-, and object-selective regions of visual cortex, which closely overlap both at the group-level and within individual subjects (Downing et al., 2007). Interestingly, the MEG data showed a specific temporal profile associated with such shape-independent body representations. Response patterns between 130 and 200ms after stimulus onset allowed for successful cross-classification, in line with previous electrophysiological findings showing that bodies can be differentiated from other categories based on scalp distributions from 130 to 230 ms (Thierry et al., 2006). These fMRI and MEG results thus confirm previous studies on body-selective responses but additionally show that this selectivity is not fully explicable by 2D shape properties.

A particular strength of the cross-decoding approach used here is that it provides a rigorous control of possible visual differences between the two categories (bodies, clothes), beyond the shape matching of the two body-clothing pairs: uncontrolled visual differences in one comparison (e.g., the presence of a neck in torsos, not shirts) would also need to be present in the other comparison (e.g., hand versus glove) for these differences to lead to successful decoding. Thus, successful decoding in this analysis likely reflects genuine category membership rather than visual or shape properties. Similarly, it is unlikely that differences in the deployment of spatial attention could account for the results: classifiers picking up on such differences between the two training stimuli (e.g., a preferential allocation of attention to the upper part of torsos, but not shirts) are unlikely to benefit from this when tested on the other comparison. It is still possible, in principle, that there are remaining visual differences, such as skin texture or 3D volume, that are shared by the body conditions but not the clothes conditions. However, we think it is unlikely that such features would drive body-selective responses, considering previous work showing body-selective responses to highly schematic depictions of the body lacking these cues (e.g., point-light motion, stick figures, silhouettes; Peelen and Downing, 2007). Nevertheless, further studies are needed to identify and rule out any such remaining differences.

We interpret the present findings as showing that the presence of particular visual or shape features is not necessary for evoking a body-selective response. Rather, these responses appear to reflect (or follow from) the categorization of an object as being a body part – a category that is associated with specific perceptual and conceptual properties, such as bodily actions/movements, social relevance, and agency (Sha et al., 2014). Different cues can support the inference that a perceived object is a body. These

cues are often part of the object itself (e.g., characteristic body shapes or movements) but may also come from the surrounding context (Cox et al., 2004), from other modalities, or from expectations and knowledge (e.g., knowing that a mannequin in a shopping window is not a human). Our results show that body-selective responses in lateral occipitotemporal cortex, emerging at around 130-200ms, follow from this categorical inference rather than reflecting a purely stimulus-driven response to the visual features of the object.

Interestingly, clusters exhibiting category-independent shape responses overlapped with clusters exhibiting shape-independent category responses. This observation is congruent with previous studies highlighting both visual (Andrews et al., 2015; Baldassi et al., 2013) and semantic (Huth et al., 2012; Sha et al., 2014) dimensions as organizational principles of high-level visual cortex. Response patterns in inferotemporal cortex seem to be best explicable by models using a combination of visual feature attributes and category membership (Khaligh-Razavi and Kriegeskorte, 2014), suggesting that in high-level visual cortex these representations co-exist.

While the fMRI data demonstrated that shape and category responses are spatially entwined, the MEG results revealed differing temporal dynamics of these responses: while shape-specific responses could be decoded early and across a relatively long time interval, shape-independent category responses showed a specific temporal signature between 130 and 200ms. We interpret this as a temporally restricted period where cortical responses reflect processing of category membership: successful decoding in the category cross-decoding analysis does not only require shape-independence of body-specific responses, but also generalization across different body parts. This generalization might be restricted to the specific time window revealed here,

with earlier computations reflecting stimulus-specific attributes (related to individual body parts), and later processing reflecting more sophisticated stimulus analysis that diverges for different body parts (e.g., hands carry different social and action-related information than torsos). Hence, the temporally specific generalization across body parts observed here might reflect a unique timestamp of category-level recognition. Interestingly, this category-level recognition occurred at different time points for the two body parts included in the study, with slightly faster categorization of the hands (130-160ms) than the torso (160-200ms). This later discriminability of torsos and shirts may reflect the greater similarity of these two stimuli on a perceptual level (see Fig. 1a), leading to relatively delayed recognition of the torsos as being a body part.

To conclude, the present study characterizes the spatial and temporal profiles of shape-independent categorical neural responses by showing that MEG and fMRI response patterns distinguish between body parts and closely matched control stimuli. The patterns that distinguished each of the two body parts from their respective shape-matched controls showed sufficient commonality to allow for cross-pair decoding of object category. These generalizable category-selective response patterns were localized in space (lateral occipitotemporal cortex) and time (130-200ms after stimulus onset).

Acknowledgements

We thank Nick Oosterhof for help with data analysis.

Grants

The research was funded by the Autonomous Province of Trento, Call "Grandi Progetti 2012", project "Characterizing and improving brain mechanisms of attention - ATTEND".

References

Andrews TJ, Watson DM, Rice GE, Hartley T. Low-level properties of natural images predict topographic patterns of neural responses in the ventral visual pathway. *J Vis*, 15: 3, 2015.

Baldassi C, Alemi-Neissi A, Pagan M, Dicarlo JJ, Zecchina R, Zoccolan D. Shape similarity, better than semantic membership, accounts for the structure of visual object representations in a population of monkey inferotemporal neurons. *PLoS Comput Biol*, 9: e1003167, 2013.

Bona S, Cattaneo Z, Silvanto J. The causal role of the occipital face area (OFA) and lateral occipital (LO) cortex in symmetry perception. *J Neurosci*, 35: 731-738, 2015.

Brainard DH. The psychophysics toolbox. *Spat Vis,* 10: 433-436, 1997.

Caldara R, Seghier ML, Rossion B, Lazeyras F, Michel C, Hauert CA. The fusiform face area is tuned for curvilinear patterns with more high-contrasted elements in the upper part. *Neuroimage*, 31: 313-319, 2006.

Carlson T, Tovar DA, Alink A, Kriegeskorte N. Representational dynamics of object vision: The first 1000 ms. *J Vis*, 13: 1-19, 2013.

Cichy RM, Pantazis D, Oliva A. Resolving human object recognition in space and time. *Nat Neurosci*, 17: 455-462, 2014.

Cox D, Meyers E, Sinha P. Contextually evoked object-specific responses in human visual cortex. *Science*, 304: 115-117, 2004.

Downing PE, Wiggett AJ, Peelen MV. Functional magnetic resonance imaging investigation of overlapping lateral occipitotemporal activations using multi-voxel pattern analysis. *J Neurosci*, 27: 226-233, 2007.

Downing PE, Jiang Y, Shuman M, Kanwisher N. A cortical area selective for visual processing of the human body. *Science*, 293: 2470-2473, 2001.

Formatted: German

Gauthier I, Tarr MJ, Movlan J, Skudlarski P, Gore JC, Anderson AW. The fusiform "face area" is part of a network that processes faces at the individual level. *J Cogn Neurosci*, 12: 495-504, 2000.

Haxby JV, Gobbini MI, Furey ML, Ishai A, Schouten JL, Pietrini P. Distributed and overlapping representations of faces and objects in ventral temporal cortex. *Science*, 293: 2425-2430, 2001.

Huth AG, Nishimoto S, Vu AT, Gallant JL. A continuous semantic space describes the representation of thousands of object and action categories across the human brain. *Neuron*, 76: 1210-1224, 2012.

Julian JB, Fedorenko E, Webster J, Kanwisher N. An algorithmic method for functionally defining regions of interest in the ventral visual pathway. *Neuroimage*, 60: 2357-2364, 2012.

Kanwisher N, McDermott J, Chun MM. The fusiform face area: a module in human extrastriate cortex specialized for the perception of faces. *J Neurosci*, 17: 4302-4311, 1997.

Kaiser D, Oosterhof NN, Peelen MV. The temporal dynamics of target selection in real-world scenes. *J Vis*, 15: 740, 2015.

Khaligh-Razavi S-M, Kriegeskorte N. Deep supervised, but not unsupervised, models may explain IT cortical representation. *PLoS Comput Biol*, 10: e1003915, 2014.

Kriegeskorte N, Mur M, Ruff DA, Kiani R, Bodurka J, Esteky H, Tanaka K, Bandettini P. Matching categorical object representations in inferior temporal cortex of man and monkey. *Neuron*, 60: 1126-1141, 2008.

Formatted: English (UK)

Oostenveld R, Fries P, Maris E, Schoffelen J-M. FieldTrip: Open source software for advanced analysis of MEG, EEG, and invasive electrophysiological data. *Comput Intell Neurosci*, 2011: 156869, 2011.

Peelen MV, Downing PE. The neural basis of visual body perception. *Nat Rev Neurosci,* 8: 636-648, 2007.

Sha L, Haxby JV, Abdi H, Guntupalli JS, Oosterhof NN, Halchenko YO, Connolly AC. The animacy continuum in the human ventral vision pathway. *J Cogn Neurosci*, 37: 665-678, 2015.

Smith SM, Nichols TE. Threshold-free cluster enhancement: Addressing problems of smoothing, threshold dependence and localisation in cluster inference. *Neuroimage*, 44: 83-98, 2009.

Thierry G, Pegna AJ, Dodds C, Roberts M, Basan S, Downing PE. An event-related potential component sensitive to images of the human body. *Neuroimage*, 32: 871-879, 2006.

Figure Legends

Fig. 1. Stimuli and Paradigm. a) The stimulus set contained two human body parts (hands and torsos; see first and third row for examples), and two pieces of clothing that are highly similar in their shape (gloves and shirts; second and fourth row). b) Stimuli were presented for 500ms, separated by a variable 1500 – 2000ms fixation interval. Participants were instructed to maintain central fixation and to manually respond to chairs.

Fig. 2. Shape cross-decoding analysis. To reveal shape-selective mechanisms, classifiers were trained to discriminate shape within one category (e.g. hands versus torsos), and tested on the other category (e.g. gloves versus shirts). Results from both train/test directions were averaged. a,b) fMRI decoding was significantly above chance in large areas of visual cortex, spanning primary visual areas and regions of occipitotemporal cortex. c) MEG decoding was significantly above chance along the diagonal, starting from 90ms after stimulus onset and peaking after 170ms and 240ms. Note that the axes here reflect time with respect to the two possible train and test comparisons, independently of the actual train/test-direction. The connected area indicates above-chance decoding.

Fig. 3. Category cross-decoding analysis. To reveal generalization across the two body-clothes pairs, classifiers were trained on one comparison (e.g. hands versus gloves), and tested on the other (e.g. hands versus gloves). Results from both train/test directions were averaged. a) fMRI decoding was significantly above chance in bilateral regions of lateral occipito-temporal cortex. b) The clusters obtained in this searchlight analysis fell

within regions previously reported as body-selective -- the black outline represents the boundaries of a group map of body-selectivity in occipitotemporal cortex (taken from http://web.mit.edu/bcs/nklab/GSS.shtml). c) MEG decoding revealed a temporally specific window of successful cross-classification ranging from 130–160ms with respect to the hand-glove comparison ("hand time") and from 160–200ms with respect to the torso-shirt comparison ("torso time"). Note that the axes here reflect time with respect to the two possible train and test comparisons, independently of the actual train/test-direction. The connected area indicates above-chance decoding.

424 **Figure 1**

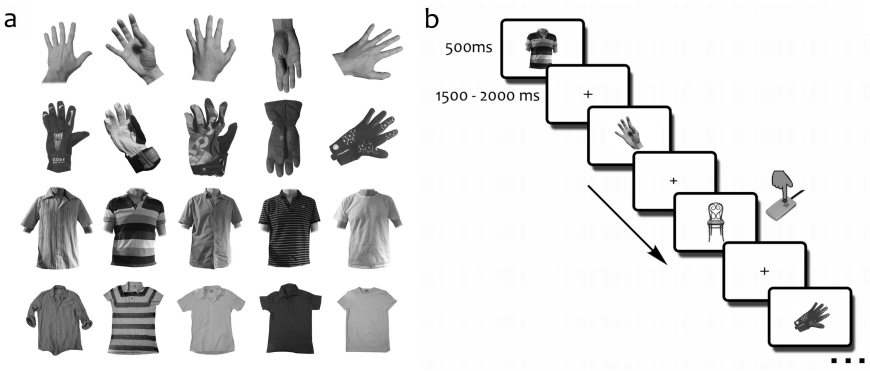

425

426

Figure 2

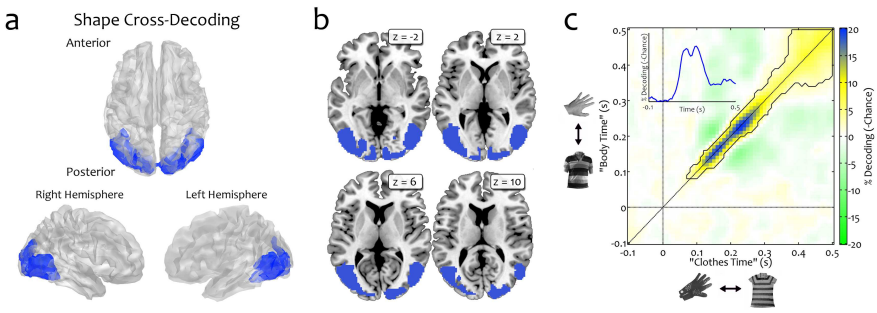
a
Shape Cross-Decoding
Anterior
Posterior
Right Hemisphere
Left Hemisphere
b
Z = -2
Z = 2
Z = 6
Z = 10
c
"Body Time" (s)
"Clothes Time" (s)
% Decoding (-Chance)
Time (s)

Figure 3

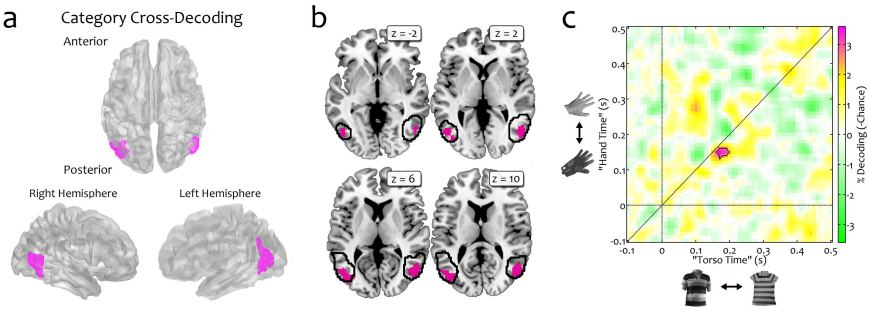
a
Category Cross-Decoding
Anterior
Posterior
Right Hemisphere
Left Hemisphere
b
z = -2
z = 2
z = 6
z = 10
c
"Hand Time" (s)
"Torso Time" (s)
% Decoding (-Chance)